Anti-c-Met antibody bioconjugated with hollow gold nanospheres as a novel nanomaterial for targeted radiation ablation of human cervical cancer cell

YING LIANG[1], JIAO LIU[2], TING LIU[1] and XINGSHENG YANG[1]

[1]Department of Obstetrics and Gynecology, Qilu Hospital, Shandong University, Jinan, Shandong 250012; [2]Department of Obstetrics and Gynecology, People's Hospital of Laiwu, Laiwu, Shandong 271199, P.R. China

Received April 14, 2016; Accepted April 21, 2017

DOI: 10.3892/ol.2017.6383

Abstract. Radiotherapy is preferred to chemotherapy as an adjuvant therapy for postoperative cervical cancer owing to its convenience and minimal effects on various non-targeted systems. The present study sought to investigate whether the utilization of anti-MET proto-oncogene, receptor tyrosine kinase (c-Met) antibodies conjugated to hollow gold nanospheres (anti-c-Met/HGNs) may enhance the efficiency of radiation therapy for cervical cancer. Anti-c-Met/HGNs were synthesized and confirmed to target c-Met, which was overexpressed on the cell membrane of multiple malignancies. The successful synthesis of HGNs was observed using transmission electron microscopy (TEM). Overrepresentation of c-Met in the human cervical cancer cell line CaSki was verified by immunofluorescence. The cellular uptake of HGNs was assessed using inductively coupled plasma atomic emission spectroscopy (ICP-AES). To assess the toxicity of functionalized gold nanospheres, a cell proliferation and toxicity assay was used and flow cytometry, with staining by propidium iodide (PI), was performed to study the cell cycle changes. Each experiment was conducted on three groups: Control, HGNs alone and anti-c-Met/HGNs, with each group also assessed with or without X-rays. The variation of apoptotic rate was observed by flow cytometry using a dual-staining Annexin V-fluorescein isothiocyanate/PI kit. Expression of apoptosis-associated proteins was examined by western blot analysis. TEM revealed a number of hollow spheres with cells with an average diameter of 56.25 nm and a mean wall thickness of 6.56 nm. CaSki cells were detected by inverted fluorescence microscopy via a layer of fluorescent green marker, and ICP-AES confirmed the distinct uptake of anti-c-Met/HGNs by each CaSki cell. Anti-c-Met/HGNs induced 38.7% of cells to stay in the G2/M phase, whereas the equivalent proportion in the control group was 19.8%. Compared with other groups, CaSki cells treated with anti-c-Met/HGNs and 5 Gy X-ray radiation exhibited a higher apoptosis rate (16.92%) and a higher early apoptotic rate (12.30%) compared with cells under other conditions (control+0 Gy: 3.16 and 1.69%; HGN+0 Gy: 3.98 and 1.94%; anti-c-Met/HGN+0 Gy: 3,47 and 1.85%; control+5 Gy: 5.35 and 3.66%; HGN+5 Gy: 7.91 and 4.06%). The anti-c-Met/HGN X-ray-treated group also evidently overexpressed caspase-3 and BCL2 associated X, apoptosis regulator. Anti-c-Met/HGN may, therefore, aid the sensitivity of radiation therapy in cervical cancer.

Correspondence to: Dr Xingsheng Yang, Department of Obstetrics and Gynecology, Qilu Hospital, Shandong University, 107 Wenhuaxi Road, Jinan, Shandong 250012, P.R. China
E-mail: xingshengyang@sdu.edu.cn

Key words: nanoparticle, hepatocyte growth factor receptor, radiation therapy, uterine cervical cancer, targeting therapy

Introduction

Uterine cervical cancer is the third most commonly diagnosed cancer and the fourth leading cause of cancer-associated mortality in women globally (1). For patients with early-stage cervical cancer, surgery remains the first-choice therapy. Other adjuvant therapies, including chemotherapy and radiotherapy, are also required for late-stage patients and occasionally for postoperative early-stage patients. The aim of radiation therapy is to deliver a high therapeutic dose of ionizing radiation to the tumor within the tolerance of normal tissue. Radiotherapy of uterine cervical cancer covers all cells within its radiation field, affecting cancer cells and normal tissue, particularly the pelvic organs. As traditional strategies lack targeting specificity, the study of novel agents to enhance therapeutic sensitivity is urgently required.

Gold-based nanomaterials have emerged as highly effective platforms for theranostic agents (2). An *in vitro* study in bovine aortic endothelial cells confirmed that it is possible to use gold nanoparticles to enhance the radiation dose to the cells in the kilovoltage range of X-ray beams in order to reduce the risk of side effects from superficial X-ray treatments (3). A previous study also demonstrated that gold nanoparticles increase the cytotoxicity of radiation in MCF-7 cells and decrease the local damage to normal tissue surrounding the breast cancer tissue (4).

Previous studies have demonstrated that the degree of radiosensitization was dependent on the average number of gold nanoparticles internalized within the cells (5). A

major challenge of the present study was to identify suitable tumor-specific biomarkers to conjugate to gold nanoparticles to achieve targeted delivery. MET proto-oncogene, receptor tyrosine kinase (c-Met) is the receptor for hepatocyte growth factor (HGF) (6). c-Met overexpression is associated with the proliferation, invasion and metastasis of cancer cells (7). In the study by Baykal *et al* (8), overexpression of c-Met was observed in 59.6% of invasive cervical carcinoma specimens. According to Kaplan-Meier univariate survival analysis and multivariate Cox regression analysis, the overexpression of c-Met is an independent variable for disease-free survival (8).

In the present study, HGNs with a diameter of ~56 nm were synthesized. Polyethylene glycol (PEG), which densely coats the HGN surface in order to reduce non-specific binding, is a neutral polymer (9); pegylation is a modification that imparts functionality onto the HGN, decreasing immunogenicity and the clearance rate (10). PEG complexes carrying different functional groups (carboxyl and sulfhydryl) readily conjugate to the gold surface through covalent bonds using thiol-terminated compounds, and combine to targeting antibodies by forming amide bonds. The present study investigated whether anti-c-Met/HGNs enhanced cytotoxicity on cervical cancer cells undergoing X-ray radiation therapy *in vitro,* and the underlying mechanisms were studied.

Materials and methods

Synthesis of HGNs. A total of 180 mg silver nitrate (Aladdin Chemistry Co., Ltd. Shanghai, China) was dissolved in 100 ml deionized water under rigorous stirring. High-purity nitrogen was then passed into the solution to create a nitrogen atmosphere which was maintained during the whole reaction. Following rapid heating to boiling point, 1 ml 1% sodium citrate (Aladdin Chemistry Co., Ltd.) was added to the reaction solution and the solution was heated to boil for another 30 min, following which the solution was cooled to ambient temperature. Hollow gold nanospheres were prepared using the galvanic replacement reaction between $HAuCl_4$ and colloidal silver in an aqueous solution under refluxing conditions, as follows. A total of 10 ml silver colloid was added to a 50 ml flask under magnetic stirring and then heated to 60˚C. Meanwhile, an aqueous solution of 5 ml $HAuCl_4$ (1 mM, Sigma-Aldrich; Merck KGaA, Darmstadt, Germany) was slowly added to the flask through a syringe pump at a rate of 45 ml/h under magnetic stirring. The solution was heated for 30 min and concentrated at 5,000 x g at room temperature for 5 min following this. The HGNs was characterized by ultraviolet-visible-near infrared (UV-Vis-NIR) spectrophotometry and transmission electron microscopy (TEM; JEM-1011; JEOL, Ltd., Tokyo, Japan).

Synthesis of anti-c-Met/HGNs. A total of four sub-steps were involved in anti-c-Met/HGN synthesis. First, to synthesize PEG Mixtures, 0.017 g methoxy polyethylene glycol carried with sulfhydryl (Shanghai Yare Biotech, Inc., Shanghai, China) and 0.003 g carboxymethyl-PEG-thiol (Shanghai Seebio Biotech, Inc., Shanghai, China) were dissolved in 2 ml double-distilled water. Second, to synthesize PEG-HGNs, 200 μl 10 nM HGN solution was added to 200 μl of the previously prepared PEG mixture, and the solution was mixed at 4˚C for 8 h. Third, for functionalization of the carboxyl group, 30 min following the addition of 5 μl 1-ethyl-3-(3-dimethylaminopropyl) carbodiimide (40 mg/ml) and N-hydroxysuccinimide (60 mg/ml) into the aforementioned PEG-HGN dispersion at room temperature, the solution was concentrated at 9,000 x g at room temperature for 5 min. Next, the supernatant was discarded and double-distilled water added to a final volume of 200 μl. Fourth, to synthesize anti-c-Met/HGNs, 3 μl anti-c-Met antibody (cat. no. EP1415Y, Abcam, Cambridge, MA, USA) was added to the solutions at room temperature for 2 h, then incubated at 4˚C for 8 h. The absorbance of anti-c-Met/HGNs was examined by UV-Vis-NIR spectrophotometry at 300-900 nm wavelength.

Cell line and culture conditions. The human cervical cancer CaSki cell line was purchased from the American Type Culture Collection (Manassas, VA, USA). Cells were cultured in RPMI 1640 medium (Gibco; Thermo Fisher Scientific, Inc., Waltham, MA, USA) with 10% mycoplasma-free fetal bovine serum (FBS) (Gibco; Thermo Fisher Scientific, Inc.) plus 1% streptomycin/penicillin (Beijing Solarbio Science & Technology Co., Ltd., Beijing, China). Cells were incubated in a CO_2 incubator (HF240; Shanghai Lishen Scientific Equipment Co., Ltd., Shanghai, China) under standardized conditions (37˚C, 5% CO_2, 100% humidity). The medium was changed 2-3 times a week.

Immunofluorescent staining. CaSki cells were seeded on 15-mm microscope cover glass slides. Following an overnight incubation under standardized conditions (37˚C, 5% CO_2, 100% humidity), cells were fixed with 4% paraformaldehyde for 15 min, washed three times with PBS, and cells were blocked with normal goat serum (Bosterbio Co., Ltd., Wuhan, China) for 30 min at room temperature. Following this, the cells were incubated with anti-c-Met antibody (cat. no. EP1454Y; 1:500 dilution; Abcam) in a wet box overnight at 4˚C. Following three PBS washes, cells were stained with Dylight 488 conjugated goat anti-rabbit IgG (A23220; 1:200 dilution; Abbkine Scientific Co., Ltd., Redlands, CA, USA) for 1 h in the dark at room temperature. The nuclei was stained with 100 μl DAPI (4',6-diamidino-2-phenylindole) staining solution (1.0 μg/ml Bosterbio Co., Ltd.) for 3 min at room temperature in the dark. The fluorescently labeled c-Met was observed and images were captured with a fluorescence inverted microscope (IX81; Olympus Corporation, Tokyo, Japan).

Cell uptake of HGNs and anti-c-Met/HGNs. CaSki cells (200,000) were cultured in 25 cm^2 cell culture flasks. The complete RPMI-1640 medium was replaced with FBS-free RPMI-1640 medium when cells reached 70% confluence. HGNs alone and anti-c-Met/HGNs were then added at different intervals (4, 8, 12, 24, 48 and 72 h). The cells were thoroughly washed with PBS, collected and resuspended into double-distilled water to a final volume of 1 ml. Cell counting was performed for each sample using a hemocytometer. A total of 1 ml aqua regia was dropped into each sample overnight to lyse the cells. Following this, double-distilled water was added to each sample to a final volume of 10 ml, the acid was neutralized, the particles filtered out and the gold mass of each sample was measured by inductively coupled plasma atomic emission spectroscopy.

Cytotoxicity of HGNs and anti-c-Met/HGNs. Cells were seeded in a 96-well culture plate at ~7.5x10^3 cells per well and incubated at 37˚C and 5% CO_2 overnight. The original complete RPMI-1640 medium was then replaced with FBS-free RPMI-1640 medium containing different concentrations (ranged from 0.0-3.3 nM) of HGNs and anti-c-Met/HGNs for 24 h. Following three washes with PBS, fresh medium containing 10% FBS was added to each well. Cell viability was measured using a Cell Counting Kit-8 (CCK-8; Nanjing Enogene Biotech Co., Ltd., Nanjing, China) assay based on the optical density value of the cells in each well at a 450 nm wavelength. Next, 10 μl of CCK-8 reagent was added into each well and cells were incubated for an additional 2 h at 37˚C. The results were determined using a microplate reader (Bio-Rad Laboratories, Inc., Hercules, CA, USA) measuring the absorbance at 450 nm. The cell viability of each group was calculated using GraphPad Prism version 7.0 (GraphPad Software, Inc., La Jolla, CA, USA). The experiment was performed in triplicate.

Cell cycle assay. Subsequent to culturing with anti-c-Met/HGNs for 24 h, cells were fixed using 70% cold ethanol overnight at 4˚C. Following two washes with cold PBS, cells were resuspended and treated with 10 μg/ml RNase for 30 min at 37˚C, cells were stained with 200 μl propidium iodide (PI; 50 μg/ml) for 30 min at 4˚C. Analysis was performed using a FACS Calibur flow cytometer (BD Biosciences, San Jose, CA, USA). Experiments were performed in triplicate. For each sample, 5,000 cells were measured. The data on cellular DNA content and cell cycle were analyzed using FlowJo v.10.0 software (Tree Star, Inc., Ashland, OR, USA).

Radiation cytotoxicity assay. Cells were seeded and incubated as aforementioned. Cells were incubated with HGNs and anti-c-Met/HGNs at laddered concentrations. An equal volume of RPMI 1640 medium was added to the control group. After 24 h, cells were washed twice with PBS, and fresh medium with 10% FBS was added. The cells were then divided into three groups: Control, HGNs and anti-c-Met/HGNs. Cells were irradiated with 6 MeV X-rays from a medical electron linear accelerator (Primus; Siemens AG, Munich, Germany) at various radiation doses (0, 2.5, 5, 7.5 and 10 Gy). The distance between the source and the cells was 25 cm. Following irradiation, cells were incubated at 37˚C until they were analyzed. Cell viability was measured 8 h following irradiation using the aforementioned CCK-8 assay. All experiments were performed in triplicate.

Cell apoptosis assay. Cell apoptosis analysis was measured by flow cytometry using a Fluorescein Isothiocyanate (FITC) Annexin V Apoptosis Detection kit I (BD Biosciences, San Jose, CA, USA) according to the manufacturer's protocol. Cells were seeded in a 6-well plate and treated with 5 Gy radiation using a 6 MeV X-ray. After 3 h, cells were harvested using EDTA-free trypsin and resuspended in 100 μl 1x binding buffer (diluted 10x binding buffer from the kit with ddH_2O to 1x binding buffer). Following the adjustment of cell numbers in each sample to an appropriate density, 5 μl FITC Annexin V and 5 μl PI were added. Another 200 μl binding buffer was added following incubation for 15 min at room temperature in the dark. Flow cytometry was conducted on a FACSCalibur flow cytometer (BD Biosciences, San Jose, CA, USA) immediately following this. Data analysis was performed using FlowJo v.10.0 software (Tree Star, Inc.). Experiments were conducted in triplicate.

Western blot analysis. Cells were cultured for 48 h following irradiation and the cell proteins of each sample were then extracted using a Total Protein Extraction kit (Beyotime Institute of Biotechnology, Haimen, China) in accordance with the manufacturer's protocol. An equivalent quality of total protein (20 μg) in each sample was loaded and electrophoresed by 15% SDS-PAGE and transferred to polyvinylidene fluoride membranes. Following blocking with 5% w/v skimmed milk powder for 1 h at room temperature, blots were incubated with antibodies against caspase-3 (cat. no. 9665), B-cell lymphoma 2 (Bcl-2; cat. no. 4223) and Bcl-associated X, apoptosis regulator (Bax; cat. no. 5023; Cell Signaling Technology, Inc., Danvers, MA, USA; 1:1,000 dilution) overnight at 4˚C. The internal control was GAPDH (cat. no. 2118; Cell Signaling Technology, Inc., Danvers, MA, USA; 1:1,000 dilution). Protein-bound membranes were then incubated with horseradish peroxidase-conjugated goat anti-rabbit secondary antibodies (cat. no. 7074; Cell Signaling Technology, Beverly, MA, USA; 1:2,000 dilution) for 1 h at room temperature. Bands were visualized by enhanced chemiluminescence (EMD Millipore, Billerica, MA, USA) using an ImageQuant LAS 4000 mini (General Electric Company, Boston, MA, USA).

Statistical analysis. Statistical analysis was performed using SPSS 17.0 (SPSS, Inc., Chicago, IL, USA). Quantitative data were expressed as the mean ± standard deviation. One-way analysis of variance and Student-Newman-Keuls tests were used. $P<0.05$ was considered to indicate statistical significance.

Results

Characterization of HGNs and anti-c-Met/HGNs. The HGNs synthesized possessed a homogeneous morphology (Fig. 1A), a mean diameter of 56.25±6.13 nm and an average wall thickness of 6.56±1.33 nm, as measured using TEM. A redshift of the plasma resonance peak occurred following the modification of naked HGNs (Fig. 1B).

Uptakes of HGNs and anti-c-Met/HGNs. HGNs are known to be taken into cancer cells by endocytosis (11). CaSki cells internalized more anti-c-Met/HGNs than naked HGNs at each time interval. Peak uptake concentration for naked HGNs and anti-c-Met/HGNs was observed at 24 h. Following incubation with the nanoparticles for 24 h, the average numbers of the nanoparticles internalized by each cell was 5,378±401 for naked HGNs and 8,681±742 for anti-c-Met/HGNs (Fig. 1C).

Fluorescence measurements. c-Met is a receptor tyrosine kinase that is a functional receptor for HGF. c-Met is a member of one of the membrane protein superfamilies, the tyrosine kinase family of growth-factor receptors, whose expression is associated with proliferation, morphogenesis and suppression of apoptosis (12). Overexpression of c-Met has been observed in different pathological types of cervical

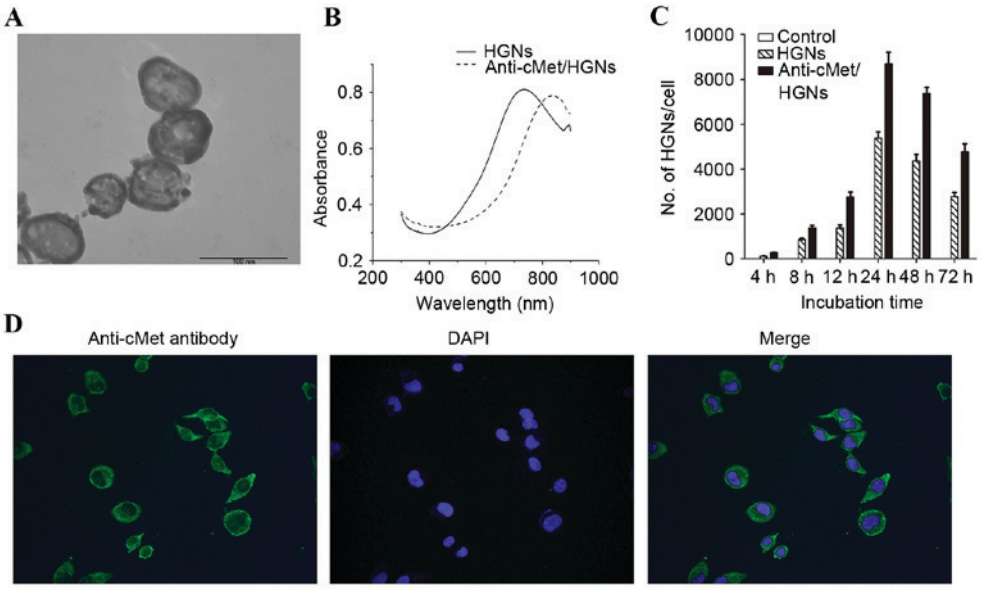

Figure 1. Characteristics of HGNs and CaSki cells. (A) Transmission electron microscope images of HGNs. (B) The resonance peak of HGNs shifts from 733 nm to 837 nm following modification with the anti-c-Met antibody. (C) The numbers of nanospheres endocytosed by each cell was counted by inductively coupled plasma atomic emission spectroscopy. The average numbers of the nanoparticles internalized per CaSki cell was 5,378±401 for naked HGNs and 8,681±742 for anti-c-Met/HGNs, respectively (P=0.005) at 24 h. (D) Immunofluorescence demonstrated that CaSki cells overexpressed c-Met on cell membrane (green staining); DAPI (blue) stains the nucleus. HGN, hollow gold nanoparticle; anti-c-Met, MET proto-oncogene, receptor tyrosine kinase antibodies; DAPI, 4',6-diamidino-2-phenylindole.

cancer (8). Immunofluorescence analysis was used to verify the presence of a layer of green fluorescent staining on the cell membrane of CaSki cells, indicating the overexpression of c-Met (Fig. 1D).

Cytotoxicity of HGNs and anti-c-Met/HGNs. Cells were incubated with either naked HGNs or anti-c-Met/HGNs at increasing concentrations, and the cytotoxicity of the nanospheres was measured by a CCK-8 test. Every condition was conducted in triplicate. The half maximal inhibitory concentration (IC_{50}) for naked HGNs in CaSki cells was 2.7 nM (Fig. 2A). PEG passivation of HGN surfaces was performed to minimize cytotoxicity. Following the incubation of CaSki cells with 2 nM HGN or anti-c-Met/HGN the cell survival rate was 65.92±3.19% for those treated with HGNs alone and 93.39±4.92% for those treated with anti-c-Met/HGNs (Fig. 2A).

Cell cycle assay. Cells were incubated with 3 nM HGNs or anti-c-Met/HGNs for 24 h. Compared with the control group, the group co-cultured with anti-c-Met/HGNs exhibited an increase in the number of cells in the G2/M phase and fewer cells in the G0/G1 phase (Fig. 2B). In the control group, the amount of cells in the G2/M phase was 19.8%, which increased to 38.7% in cells treated with anti-c-Met/HGN, a significant difference (P<0.05). Correspondingly, the ratio of cells in the G0/G1 phase in these groups was 52.0 and 46.8%, respectively. HGNs arrested cancer cells at the G2/M phase, which is the most radiosensitive phase in the cell cycle (13), and thus increased the radiation sensitivity of cancer cells.

Radiation cytotoxicity assay. Treatment with anti-c-Met/HGNs enhanced radiation sensitivity of CaSki (Fig. 3A). Compared with groups treated with X-ray radiation alone, those treated with anti-c-Met/HGNs exhibited a markedly higher cellular proliferation inhibition rate. X-ray irradiation alone (5 Gy) induced an inhibition rate of 13.2±2.5%, whereas incubation with naked HGNs (1.0 nM) with X-ray irradiation increased the inhibition rate to 37.3±6.3% and incubation with 1.0 nM anti-c-Met/HGNs with irradiation increased it further to 52.0±3.8%. A significant enhancement in inhibition rate was observed, averaging 38.7% (P<0.05) compared with controls.

Cell apoptosis assay. Flow cytometry was used to determine cell apoptosis 3 h following radiation. The flow cytometry graphs were sectioned into four quadrants. Dual staining with FITC Annexin V and PI was used to identify early apoptotic cells (Annexin V-positive, PI-negative; lower-right quadrant), viable cells (Annexin V-negative, PI-negative; lower-left quadrant) and late apoptotic together with dead cells (Annexin V-positive, PI-positive; upper-right quadrant). The results revealed that the total cell apoptotic rates of the anti-c-Met/HGNs with X-ray group was significantly higher than that of the negative control group in CaSki cells (P<0.05; Fig. 3B).

Western blot analysis. The expression of Bcl-2, caspase-3 and Bax was assessed by western blot analysis to verify the overexpression of apoptosis-related proteins (Fig. 4). The results demonstrated that the expression of proteins associated with apoptosis, including Bax and caspase-3, were increased, whereas the expression of Bcl-2 was markedly decreased in cells incubated with anti-c-Met/HGNs and treated with radiation, compared with other groups. The results indicated that X-ray irradiation may induce apoptosis in CaSki cells by disturbing the balance between Bax and Bcl-2, as well as intervening in the Fas ligand pathway.

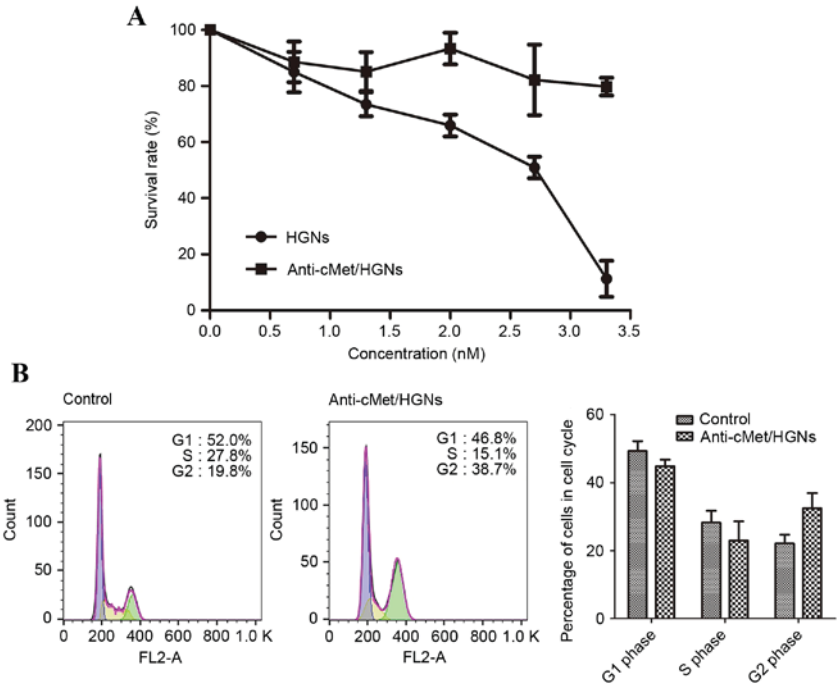

Figure 2. Cytotoxicity of nanospheres and the changes to the cell cycle induced by them. (A) The cytotoxicity of the nanospheres at a range of concentrations, as assessed using Cell Counting Kit-8. (B) Flow cytometry analysis of cell-cycle distribution, with quantification. HGN, hollow gold nanoparticle; anti-c-Met, MET proto-oncogene, receptor tyrosine kinase antibodies.

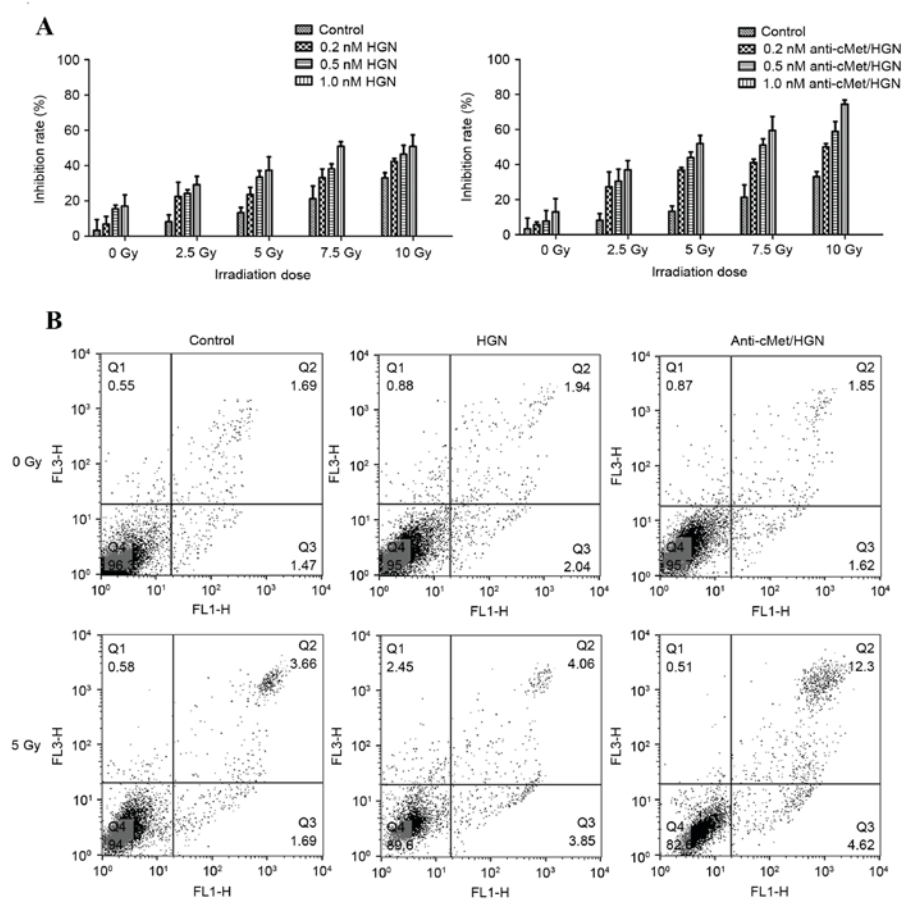

Figure 3. The inhibition and apoptosis rates of each group. (A) The inhibition rate of radiation was measured using a cell counting and apoptosis assay. Following X-ray radiation, the inhibition rate of radiation alone was 13.2±2.5%, that of naked HGNs with radiation was 37.3±6.3% and that of anti-c-Met/HGNs with radiation was 52.0±3.8%. (B) Flow cytometry was used to determine cell apoptosis following radiation. Cells were double-labeled with annexin V and propidium iodide. The results revealed that the total cell apoptosis rates in anti-c-Met/HGNs with X-ray group is higher than other groups. HGN, hollow gold nanoparticle; anti-c-Met, MET proto-oncogene, receptor tyrosine kinase antibodies.

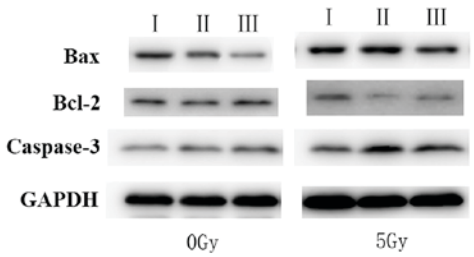

Figure 4. The expression of apoptosis-associated proteins Bax, Bcl-2 and caspase-3 by western blot analysis. I, HGNs; II, anti-c-Met/HGNs; III, control. Bax, Bcl-associated X, apoptosis regulator; Bcl-2, B-cell chronic lymphocytic leukemia/lymphoma 2.

Discussion

As it is the most common gynecologic malignancy, patients with early-stage cervical cancer ordinarily have good prognosis when they undergo radical surgery. Nevertheless, patients exhibiting high-risk features identified on pathologic examination who undergo surgery, patients with larger early-stage tumors (IB2 and IIA, diameter of >4 cm) and patients with advanced-stage tumors (IIB-IVA), which were classified according to International Federation of Obstetrics and Gynecology stage (1995) are administered radiation therapy to eliminate the tumor foci or to reduce the risk of relapse (14). The emergence of radioresistance reduces the effectiveness of radiation therapy, meaning that a novel agent is required to enhance sensitivity and to improve targeting specificity.

Nanotechnology is an emerging technique that is used to improve cellular targeting and sensitivity to radiation therapy (2). HGNs are novel therapeutic agents which possess biocompatibility, ease of synthesis and modification, and a high Z-coefficient, indicating a strong therapeutic potential (15). HGNs have been demonstrated to enhance sensitivity to radiotherapy by altering the cell-cycle distribution, and a great deal of progress has been made in designing HGN-conjugating agents for targeted radiotherapy against malignant tumors (16,17). HGNs have a high atomic number, which leads to a greater absorption of X-rays than standard agents. HGNs are also able to bind multiple proteins that are targeted to cell-surface receptors, which are overexpressed in cancer cells (18). The size and shape of gold nanoparticles alters their cellular uptake and biomedical applications. Chithrani *et al* (19) investigated the features of gold nanoparticles synthesized at a range of sizes (1-100 nm diameter) and shapes (1:1 to 1:5 aspect ratio). The authors revealed that the cellular uptake of nanoparticles was dependent on the size. The maximum uptake occurred at a size of 50 nm. A study by Osaki *et al* (20) suggested that endocytosis is highly size-dependent, as 50-nm nanoparticles entered cells via endocytosis more efficiently than smaller ones. These results suggested the optimal size of nanoparticles is ~50 nm.

In the present study, HGNs of 56.25±6.13 nm in diameter and 6.56±1.33 nm in wall thickness were synthesized through a galvanic replacement reaction using colloidal silver as the sacrificial template and $HAuCl_4$ as the precursor to gold under refluxing conditions. OPSS-PEG-NHS was used to modify HGNs to reduce their cytotoxicity, impart biocompatibility and extend blood circulation time. The PEG-coated HGNs were conjugated to anti-c-Met monoclonal antibodies, as c-Met has been confirmed to be overexpressed in different pathological categories of cervical cancer by histopathology (8). Using immunofluorescent staining, c-Met was revealed to be overexpressed on the surface of CaSki cells. The bioconjugation of the anti-c-Met antibody to HGN led to a slight red shift in the infrared absorption peak of nanospheres.

One major challenge in the field of nanoparticle therapy is the identification of an appropriate concentration of nanoparticles to minimize toxicity and maximize therapeutic efficacy. Owing to the toxicity and low biological compatibility, a high dose of naked gold nanospheres may cause severe cytotoxic responses. In the present study, uptake concentrations of nanoparticles reached peak levels at 24 h and then diminished. The cytotoxicity of HGNs was therefore assessed using different HGN concentrations following incubation for 24 h. The IC_{50} of naked HGNs was 2.7 nM in CaSki cells. As the naked HGN and antibody-conjugated HGN groups were being used, the experimental concentration used for the following experiments with radiation therapy was 1.0 nM.

Owing to their ability to reduce the effective dose of radiation, radiation sensitizers are of high clinical value. Metallic materials have been reported to arrest the cell cycle at the most radiosensitive phase (G2/M phase) to enhance the sensitivity of cancer cells towards radiation (13,21). The present study confirmed that the HGNs synthesized caused CaSki cells to accumulate at the G2/M phase. A previous study on nanotechnology also revealed the potential for enhanced tumor destruction by radiation therapy (3). Garnica-Garza *et al* (22) examined the feasibility of using X-ray beams to treat prostate cancer loaded with gold nanoparticles and the effect of the nanoparticle concentration. The present study was performed with 6 MeV X-ray energies at various radiation doses (0, 2.5, 5, 7.5 and 10 Gy). The distance of the cells from the radiation source was 25 cm and the effect of radiation was tested by the CCK-8 assay. The enhancement of radiation sensitivity for anti-c-Met/HGNs is presented in Fig. 3A.

HGNs were confirmed to mediate the radiation effect on CaSki cells using double-labeled Annexin V and PI. Annexin V staining precedes the loss of membrane integrity, which accompanies the late stages of cell death that results from either apoptotic or necrotic processes. Treatment with X-rays alone or naked HGNs with X-rays had no significant effect on cancer apoptosis rate; however, X-ray radiation in the presence of the antibody-conjugated HGNs significantly increased the apoptotic rate compared with that of the control group ($P<0.05$). Furthermore, the expression of apoptosis-associated proteins 48 h following X-ray radiation was also probed. It has been suggested that an interaction between the Fas pathway and Bcl-2 family members may define the rate of apoptosis (23). Once Fas has been activated, other downstream effector caspases, such as caspase-3, are motivated to initiate the execution phase of apoptosis (24). In the present study, the expression of Bax and caspase-3 were significantly elevated and that of Bcl-2 was significantly decreased in cells treated with anti-c-Met-conjugated HGNs and X-ray radiation, compared with radiation alone and with naked HGNs and radiation (Fig. 4). Therefore, X-ray radiation

is likely to have induced apoptosis in CaSki cells by disrupting the balance between Bcl-2 and Bax and activating the Fas signaling pathway.

The present study indicated that, compared with conventional radiotherapy strategies, low-dose X-ray radiation combined with anti-c-Met/HGN treatment is a promising therapeutic approach for the targeted elimination of cervical cancer cells. Further work will also be required to assess the functionality of HGNs in animal models and make them suitable for clinical use.

The HGNs described in the present study exhibited potential in radiation therapy for tumor ablation. The anti-c-Met/HGNs synthesized in the present study form part of a novel therapeutic approach for the targeted elimination of cervical cancer cells. Future work will also be required to ensure functionality of HGNs in animal models to make them suitable for clinical employment.

Acknowledgements

The present study was financially supported by the National Natural Science Foundation of China (grant no. 81372809), the National Clinical Research Center for Gynecological Oncology (grant no. 2015BAI13B05) and the Natural Science Foundation of Shandong Province (grant no. ZR2016HB03).

References

1. Jemal A, Bray F, Center MM, Ferlay J, Ward E and Forman D: Global cancer statistics. CA Cancer J Clin 61: 69-90, 2011.
2. Daniel MC and Astruc D: Gold Nanoparticles: Assembly, supramolecular chemistry, quantum-size-related properties, and applications toward biology, catalysis, and nanotechnology. Chem Rev 104: 293-346, 2004.
3. Rahman WN, Bishara N, Ackerly T, He CF, Jackson P, Wong C, Davidson R and Geso M: Enhancement of radiation effects by gold nanoparticles for superficial radiation therapy. Nanomedicine 5: 136-142, 2009.
4. Kong T, Zeng J, Wang X, Yang X, Yang J, McQuarrie S, McEwan A, Roa W, Chen J and Xing JZ: Enhancement of radiation cytotoxicity in breast-cancer cells by localized attachment of gold nanoparticles. Small 4: 1537-1543, 2008.
5. Chithrani DB, Jelveh S, Jalali F, van Prooijen M, Allen C, Bristow RG, Hill RP and Jaffray DA: Gold nanoparticles as radiation sensitizers in cancer therapy. Radiat Res 173: 719-728, 2010.
6. Bottaro DP, Rubin JS, Faletto DL, Chan AM, Kmiecik TE, Vande Woude GF and Aaronson SA: Identification of the hepatocyte growth factor receptor as the c-met proto-oncogene product. Science 251: 802-804, 1991.
7. Birchmeier C, Birchmeier W, Gherardi E and Vande Woude GF: Met, metastasis, motility and more. Nat Rev Mol Cell Biol 4: 915-925, 2003.
8. Baykal C, Ayhan A, Al A, Yüce K and Ayhan A: Overexpression of the c-Met/HGF receptor and its prognostic significance in uterine cervix carcinomas. Gynecol Oncol 88: 123-129, 2003.
9. Wang L, Lofton C, Popp M and Tan W: Using luminescent nanoparticles as staining probes for Affymetrix GeneChips. Bioconjug Chem 18: 610-613, 2007.
10. Wang L, Zhao W and Tan W: Bioconjugated silica nanoparticles: Development and applications. Nano Res 1: 99, 2008.
11. Tsai SW, Chen YY and Liaw JW: Compound cellular imaging of laser scanning confocal microscopy by using gold nanoparticles and dyes. Sensors (Basel) 8: 2306-2316, 2008.
12. Mizuno S and Nakamura T: HGF-MET cascade, a key target for inhibiting cancer metastasis: The impact of NK4 discovery on cancer biology and therapeutics. Int J Mol Sci 14: 888-919, 2013.
13. Turner J, Koumenis C, Kute TE, Planalp RP, Brechbiel MW, Beardsley D, Cody B, Brown KD, Torti FM and Torti SV: Tachpyridine, a metal chelator, induces G2 cell-cycle arrest, activates checkpoint kinases, and sensitizes cells to ionizing radiation. Blood 106: 3191-3199, 2005.
14. Petignat P and Roy M: Diagnosis and management of cervical cancer. BMJ 335: 765-768, 2007.
15. Dorsey JF, Sun L, Joh DY, Witztum A, Kao GD, Alonso-Basanta M, Avery S, Hahn SM, Al Zaki A and Tsourkas A: Gold nanoparticles in radiation research: Potential applications for imaging and radiosensitization. Transl Cancer Res 2: 280-291, 2013.
16. Geng F, Song K, Xing JZ, Yuan C, Yan S, Yang Q, Chen J and Kong B: Thio-glucose bound gold nanoparticles enhance radio-cytotoxic targeting of ovarian cancer. Nanotechnology 22: 285101, 2011.
17. Roa W, Zhang X, Guo L, Shaw A, Hu X, Xiong Y, Gulavita S, Patel S, Sun X, Chen J, *et al*: Gold nanoparticle sensitize radiotherapy of prostate cancer cells by regulation of the cell cycle. Nanotechnology 20: 375101, 2009.
18. Jain S, Hirst DG and O'Sullivan JM: Gold nanoparticles as novel agents for cancer therapy. Br J Radiol 85: 101-113, 2012.
19. Chithrani BD, Ghazani AA and Chan WC: Determining the size and shape dependence of gold nanoparticle uptake into mammalian cells. Nano Lett 6: 662-668, 2006.
20. Osaki F, Kanamori T, Sando S, Sera T and Aoyama Y: A quantum dot conjugated sugar ball and its cellular uptake. On the size effects of endocytosis in the subviral region. J Am Chem Soc 126: 6520-6521, 2004.
21. Wilson GD: Radiation and the cell cycle, revisited. Cancer Metastasis Rev 23: 209-225, 2004.
22. Garnica-Garza HM: Contrast-enhanced radiotherapy: Feasibility and characteristics of the physical absorbed dose distribution for deep-seated tumors. Phys Med Biol 54: 5411-5425, 2009.
23. Krammer PH: CD95(APO-1/Fas)-mediated apoptosis: Live and let die. Adv Immunol 71: 163-210, 1999.
24. Slot KA, Voorendt M, de Boer-Brouwer M, van Vugt HH and Teerds KJ: Estrous cycle dependent changes in expression and distribution of Fas, Fas ligand, Bcl-2, Bax, and pro- and active caspase-3 in the rat ovary. J Endocrinol 188: 179-192, 2006.